Supplementary for:

The spatial-temporal variations of atmospheric CH_4 concentrations and urban enhancements over the northern China based on a comprehensive dataset: ground-based observations, TROPOMI, inventory and inversions

Pengfei Han[1,2*], Ning Zeng[3], Bo Yao[4], Wen Zhang[5], Weijun Quan[6], Pucai Wang[2], Ting Wang[2], Minqiang Zhou[1,2], Qixiang Cai[7,8*], Yuzhong Zhang[9,10], Ruosi Liang[9,10], Wanqi Sun[11], Shengxiang Liu[2,12]

[1]State Key Laboratory of Atmospheric Environment and Extreme Meteorology, Institute of Atmospheric Physics, Chinese Academy of Sciences, Beijing 100029, China

[2]Carbon Neutrality Research Center, Institute of Atmospheric Physics, Chinese Academy of Sciences, Beijing, China

[3]Department of Atmospheric and Oceanic Science, and Earth System Science Interdisciplinary Center, University of Maryland, College Park, Maryland, USA

[4]Department of Atmospheric and Oceanic Sciences & Institute of Atmospheric Sciences, Fudan University, Shanghai, China

[5]State Key Laboratory of Atmospheric Boundary Layer Physics and Atmospheric Chemistry, Institute of Atmospheric Physics, Chinese Academy of Sciences, Beijing, China

[6]Institute of Urban Meteorology (Key Laboratory of Urban Meteorology), China Meteorological Administration, Beijing, China

[7]State Key Laboratory of Numerical Modeling for Atmospheric Sciences and Geophysical Fluid Dynamics, Institute of Atmospheric Physics, Chinese Academy of Sciences, Beijing, China

[8]Qiluzhongke Institute of Carbon Neutrality, Jinan, China

[9]Key Laboratory of Coastal Environment and Resources of Zhejiang Province, School of Engineering, Westlake University, Hangzhou, Zhejiang, China

[10]Institute of Advanced Technology, Westlake Institute for Advanced Study, Hangzhou, Zhejiang, China

[11]Meteorological Observation Centre, China Meteorological Administration, Beijing, China

[12]Jiujiang University, Jiujiang, Jiangxi, China

[*] *Correspondence to*: Pengfei Han (pfhan@mail.iap.ac.cn); Qixiang Cai (caiqixiang@mail.iap.ac.cn)

Fig. S1 Wind rose plots at three regional sites: BJ (Beijing), XH (Xianghe), and SDZ (Shangdianzi). 3

Fig. S2 Sectoral CH_4 emissions for the North China at provincial scale in 2019 3

Fig. S3 Monthly mean CH_4 concentration enhancements of Beijing (BJ) and Xianghe (XH) compared with Shangdianzi (SDZ). 4

Fig. S4 Temporal variations of mean monthly XCH_4 (TROPOMI, TCCON) and surface CH_4 concentrations observed in XH (a, b), and correlation relationships of mean monthly XCH_4 (TROPOMI, TCCON) and surface concentrations observed by Picarro in XH during 2019-2021. 4

Fig. S5 Hourly comparisons of optimized GEOS-Chem model simulations with in-situ high-precision measurements at three sites. MB is mean bias and RMSE is mean root square error. BJ, XH, and SDZ represent Beijing, Xianghe, and Shangdianzi observations. 5

Fig. S6 Monthly comparisons of WestLake and CAMS model simulations with in-situ high-precision measurements at three sites. MB is mean bias and RMSE is mean root square error. BJ, XH, and SDZ represent Beijing, Xianghe, and Shangdianzi observations. 5

Fig. S7 Posterior and observed seasonal mean column XCH_4 concentrations from WestLake (optimized GEOS-Chem, left 2 columns) and TROPOMI (right 2 columns) for the North China in 2019 6

Fig. S8 Correlation relationships of posterior (WestLake, in x-axis) and observed (TROPOMI, in y-axis) seasonal mean column XCH_4 concentrations. 7

Fig. S9 Model posterior monthly mean column CH_4 concentrations for the North China in 2019 7

Fig. S10 Relationships of TROPOMI XCH_4 with GEOS-Chem modeled surface CH_4 in each season and annual mean in 2019. 8

Fig. S11 Relationships of TROPOMI XCH_4 with PKU-CH_4 emissions at grid levels in Shanxi Province in 2019. 8

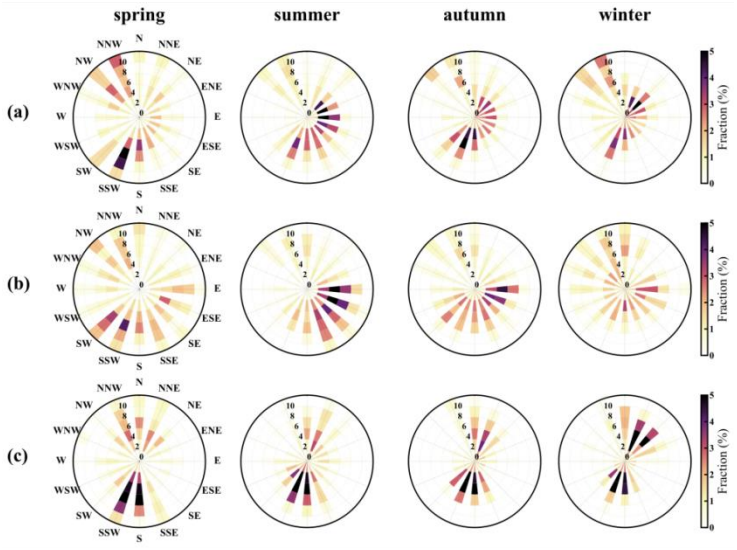

Fig. S1 Wind rose plots at three regional sites: BJ (Beijing), XH (Xianghe), and SDZ (Shangdianzi).

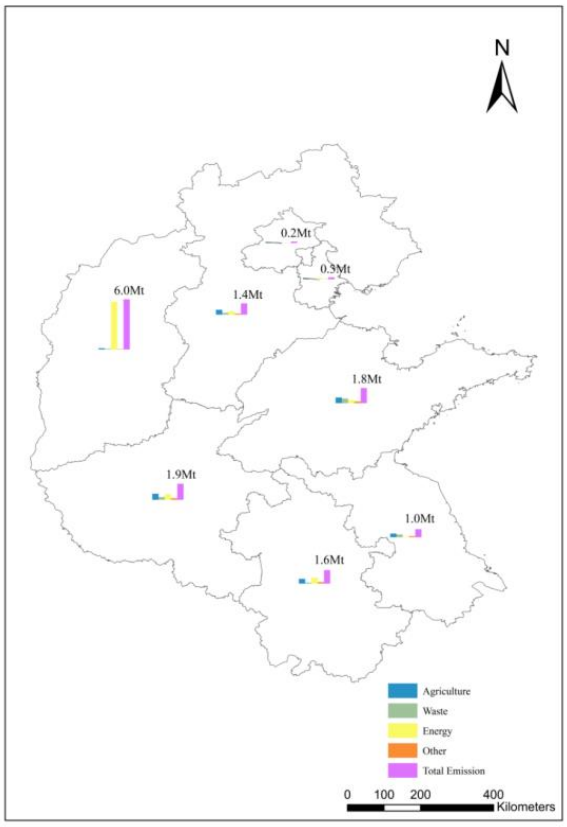

Fig. S2 Sectoral CH_4 emissions for the North China at provincial scale in 2019

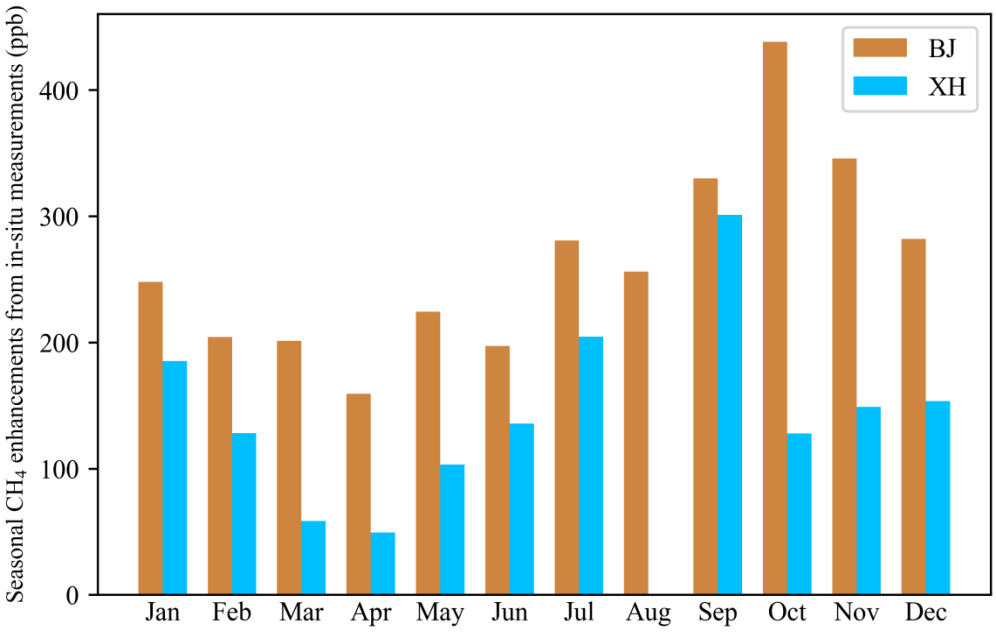

Fig. S3 Monthly mean CH_4 concentration enhancements of Beijing (BJ) and Xianghe (XH) compared with Shangdianzi (SDZ).

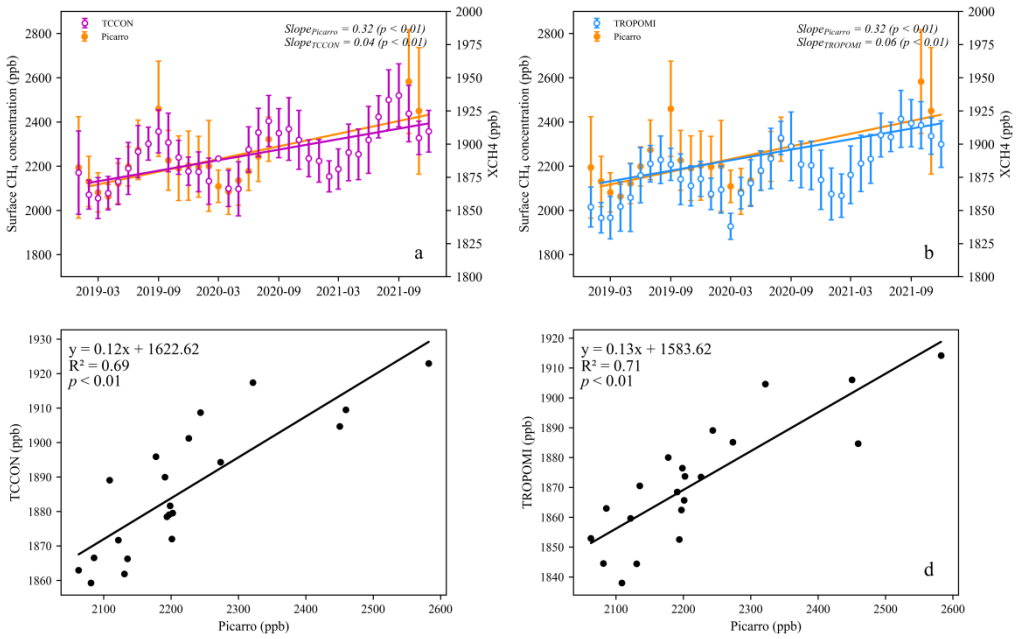

Fig. S4 Temporal variations of mean monthly XCH_4 (TROPOMI, TCCON) and surface CH_4 concentrations observed in XH (a, b), and correlation relationships of mean monthly XCH_4 (TROPOMI, TCCON) and surface concentrations observed by Picarro in XH during 2019-2021.

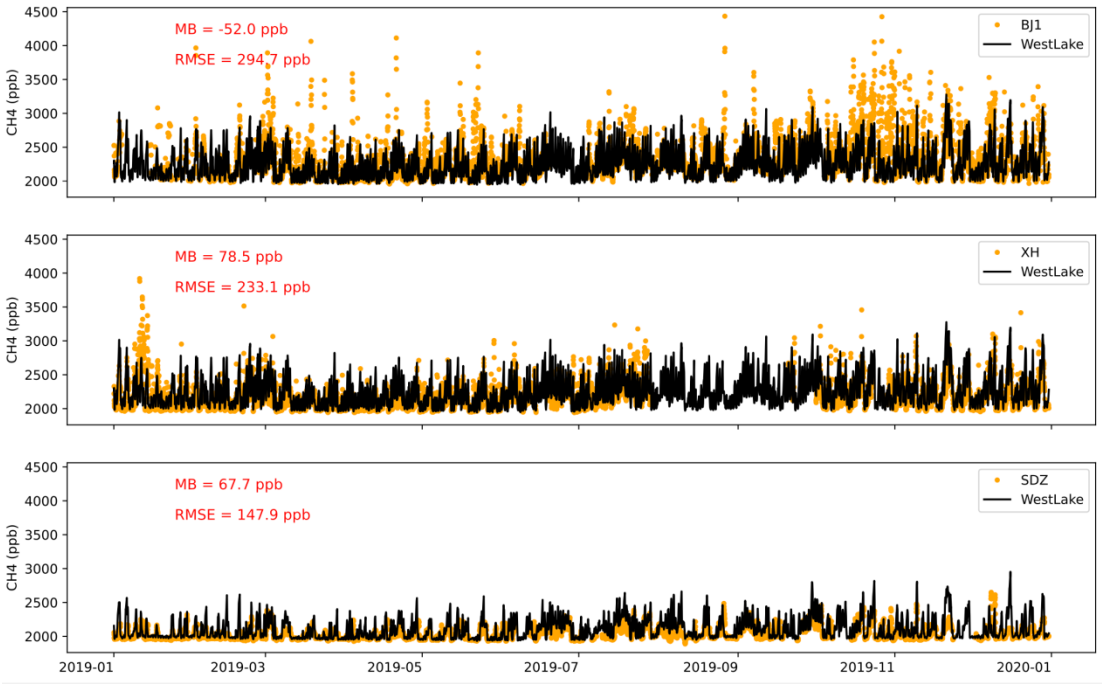

Fig. S5 Hourly comparisons of optimized GEOS-Chem model simulations with in-situ high-precision measurements at three sites. MB is mean bias and RMSE is mean root square error. BJ, XH, and SDZ represent Beijing, Xianghe, and Shangdianzi observations.

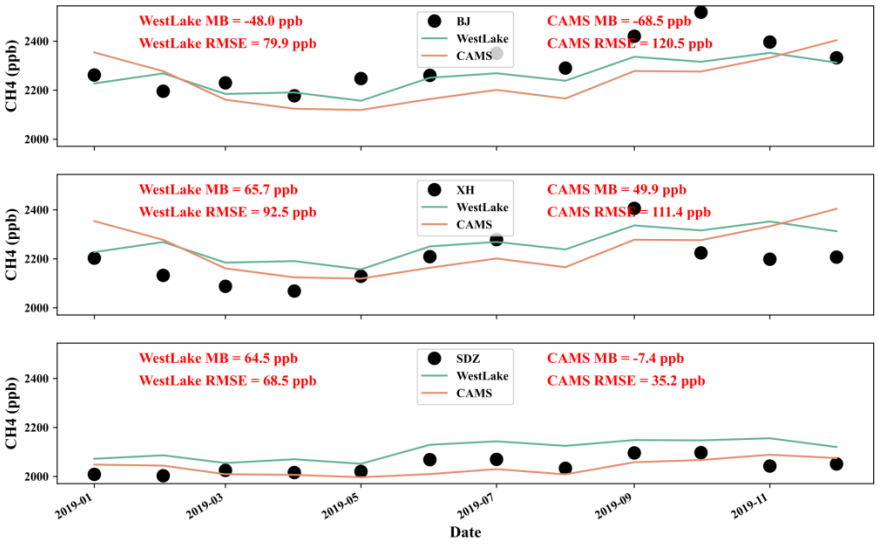

Fig. S6 Monthly comparisons of WestLake and CAMS model simulations with in-situ high-precision measurements at three sites. MB is mean bias and RMSE is mean root square error. BJ, XH, and SDZ represent Beijing, Xianghe, and Shangdianzi observations.

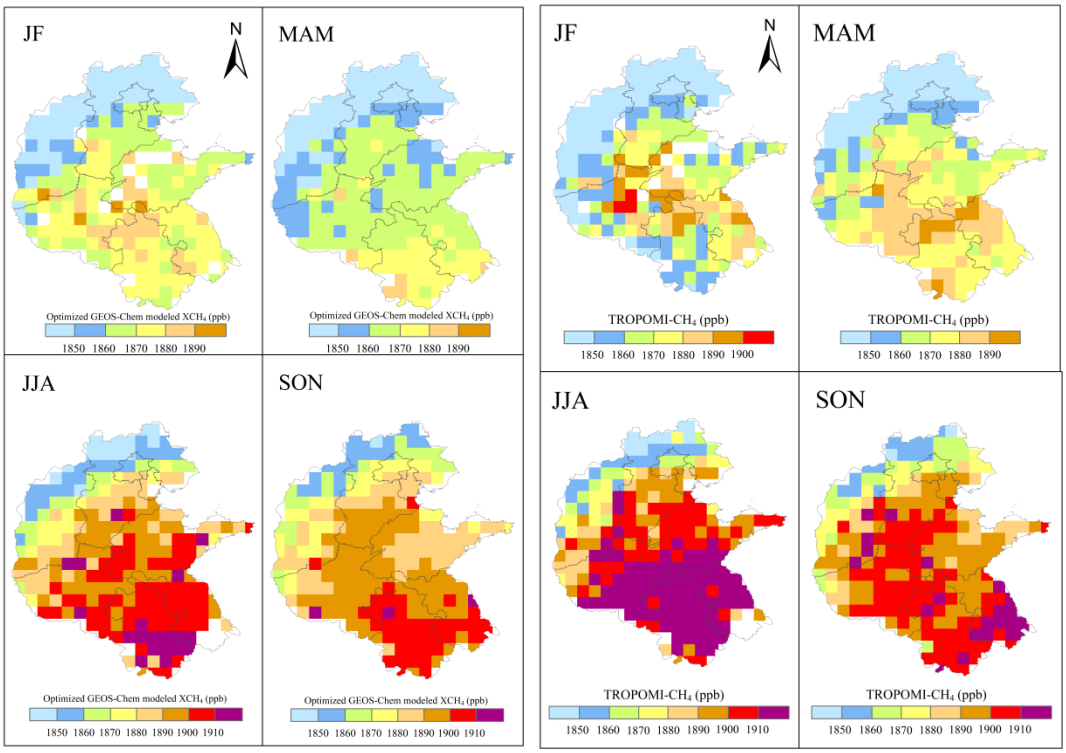

Fig. S7 Posterior and observed seasonal mean column XCH_4 concentrations from WestLake (optimized GEOS-Chem, left 2 columns) and TROPOMI (right 2 columns) for the North China in 2019

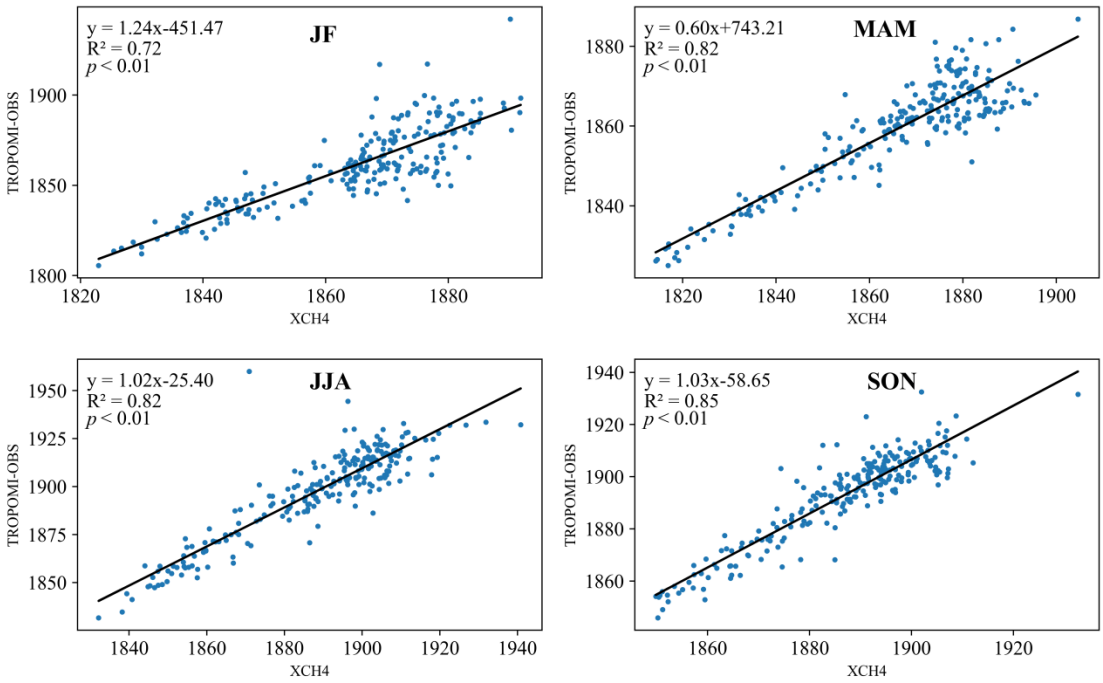

Fig. S8 Correlation relationships of posterior (WestLake, in x-axis) and observed (TROPOMI, in y-axis) seasonal mean column XCH_4 concentrations.

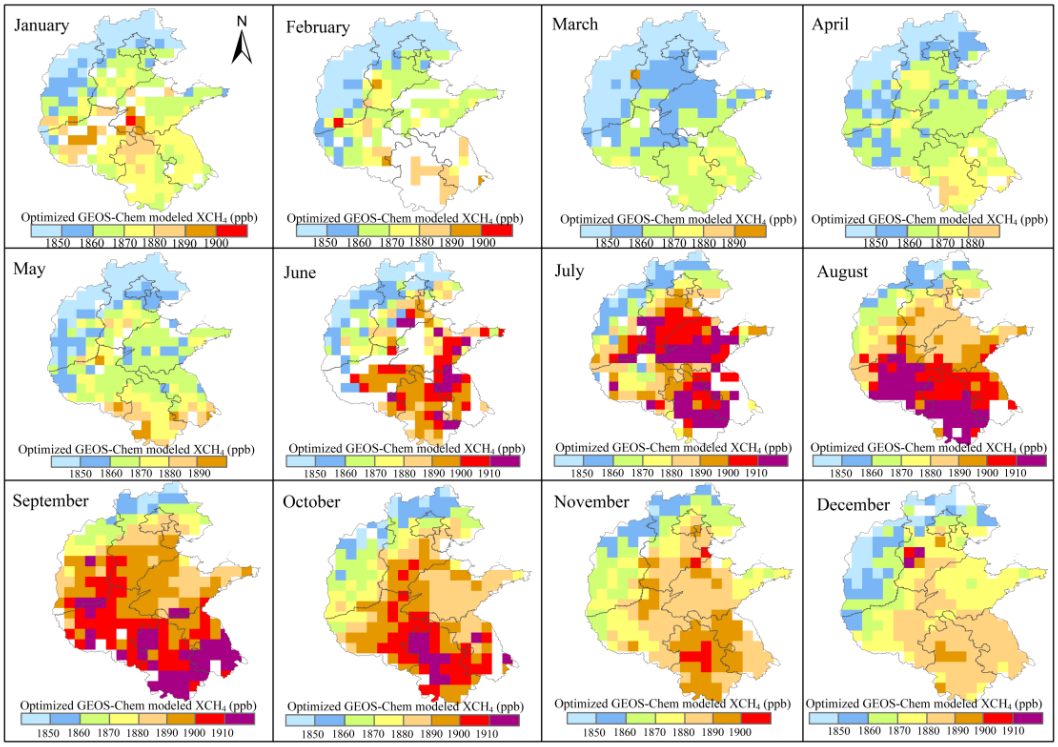

Fig. S9 Model posterior monthly mean column CH_4 concentrations for the North China in 2019

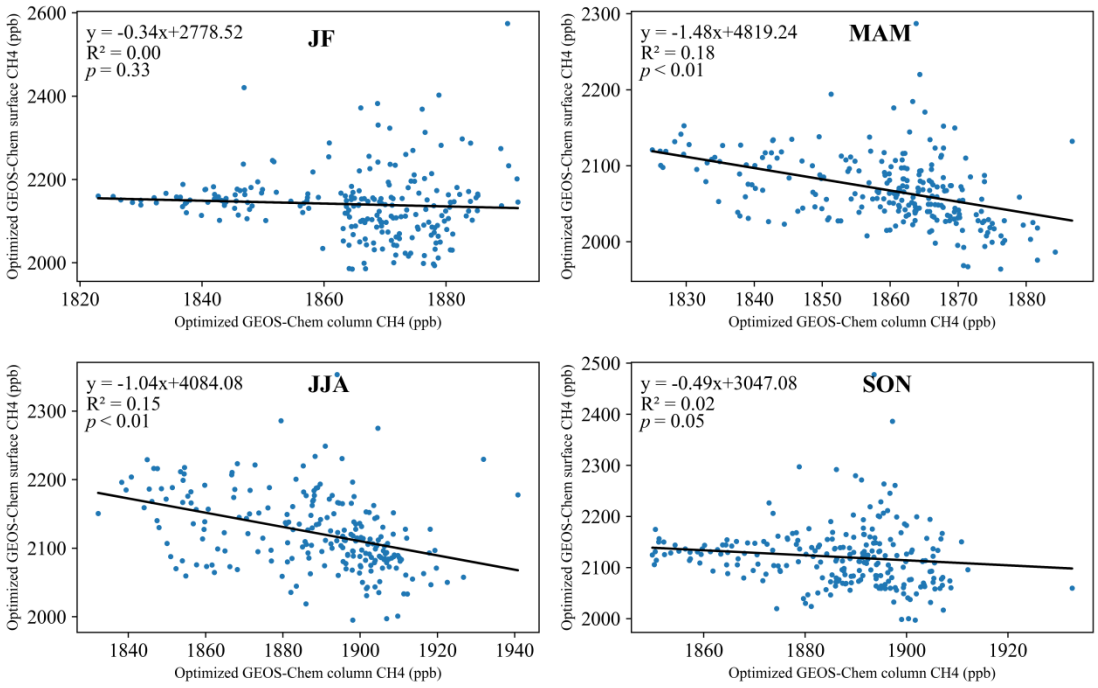

Fig. S10 Relationships of TROPOMI XCH_4 with GEOS-Chem modeled surface CH_4 in each season in 2019.

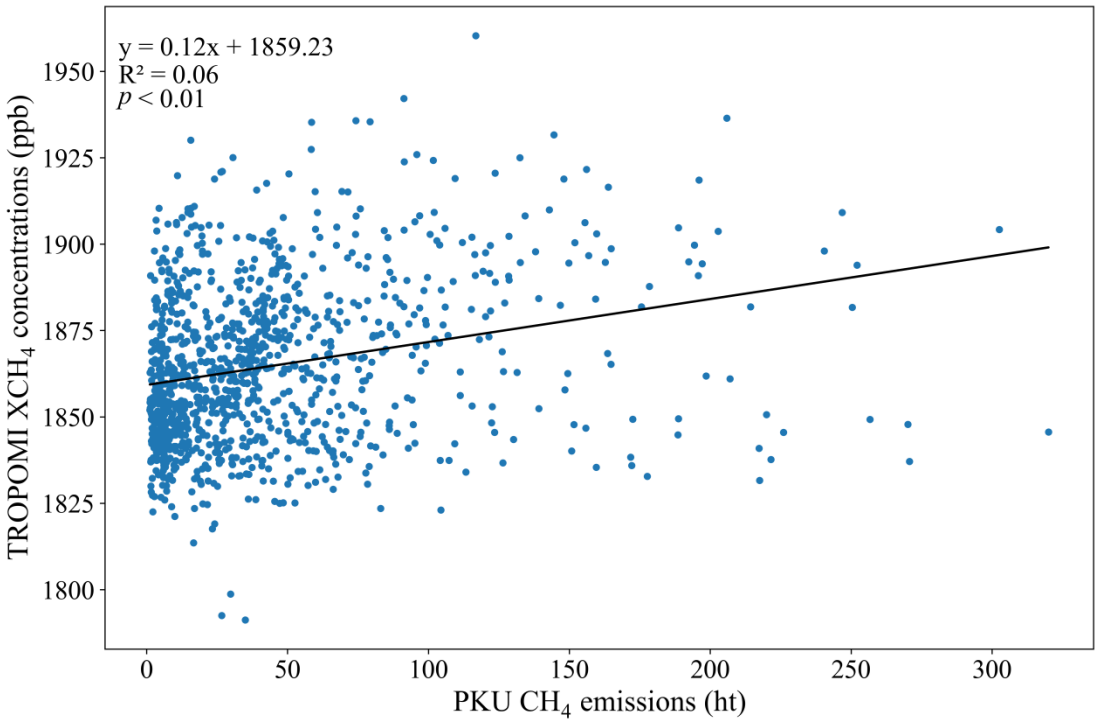

Fig. S11 Relationships of TROPOMI XCH_4 with PKU-CH_4 emissions at grid levels in Shanxi Province in 2019.